JOURNAL OF CATALYSIS 86, 254–265 (1984)

Ceria in Automotive Exhaust Catalysts

I. Oxygen Storage

H. C. YAO AND Y. F. YU YAO

Research Staff, P.O. Box 2053, Ford Motor Company, Dearborn, Michigan 48121

Received May 23, 1983; revised November 10, 1983

Oxygen storage capacities of CeO_2, CeO_2/Al_2O_3, and $PM/CeO_2/Al_2O_3$, measured by a pulse injection method, are affected by pretreatment temperature, pulsing temperature, partial pressure of CO, presence of precious metals (PM), and the concentration of CeO_2 on alumina. They are lowered by higher pretreatment temperature but increase with the pulsing temperature in the range of application. At a pulsing temperature $\leq$500°C, the capacities are not affected by oxygen pressure but increase with partial pressure of CO. The presence of PM lowers the reduction temperature and increases the oxygen storage capacity of CeO_2. TPR was used to measure the oxygen removal at various temperatures. At 900°C, the maximum amount of oxygen removed from unsupported or alumina-supported ceria is about 25%. The TPR traces of the unsupported ceria show two peaks at 500 and 750°C which are associated with the reduction of surface capping oxygen and bulk oxygen anions, respectively. For alumina-supported ceria, the TPR traces show a third peak at 850°C which is associated with the reduction of the shared oxygen anions at the interface. The presence of PM lowers only the reduction temperature of the capping oxygen anions but not of the other two oxygen species. Both oxygen chemisorption and TPR were used to measure the oxygen anion restoration at various temperatures following the reduction at 500 and 900°C, respectively. Chemisorption data show that the oxygen uptake per CeO_2 is highest at the lowest CeO_2 concentration. The TPR traces show that a new oxygen species, probably a molecular oxygen anion, is formed at 25°C which converts slowly at 500°C to the capping oxygen anion. Complete restoration of all three types of oxygen anions is accomplished at 850°C in air.

INTRODUCTION

"Oxygen storage" components of automotive catalysts are for the most part base-metal oxides capable of undergoing a relatively rapid change in oxidation state upon a change in redox potential of the exhaust gas. The change in oxidation state is associated with the reversible removal and addition of oxygen and hence the designation "oxygen storage." Ceria is one of the most commonly used components (*1*) since in addition to "oxygen storage" it imparts an improved resistance to thermal loss of BET area of the alumina support, stabilizes the active precious metals in a finely dispersed state (*2–12*), and also enhances the water–gas shift reaction for the removal of CO under O_2-deficient conditions (*13*).

As the automotive exhaust gas has a cyclic lean–rich composition fluctuation, an oxygen-storage component which readily undergoes oxyreduction cycles can provide oxygen for H_2, CO, and HC oxidation in the rich region and the reduced state can remove oxygen from the gas phase when the exhaust gas cycles into the lean region. Thus, an oxygen storage component is not only promoting the oxidation activity but also widens the air–fuel ratio window (*2, 13*) where all three major pollutants, HC, CO, and NO can be removed.

The purpose of this paper (Part 1) is to study the function and to compare the capacity of CeO_2 as an oxygen storage component in an alumina-supported precious metal catalyst.

Our preliminary work has shown that Pt or Pd can promote the reduction of CeO_2 by H_2 or CO and also its reoxidation by O_2. For O_2 and CO oxyreductions, the oxygen storage properties are investigated by pulse injection method. The factors that have influenced the behavior of ceria such as tem-

0021-9517/84 $3.00

perature, partial pressures of reactive gases, concentration and dispersion of ceria on alumina, and the effect of precious metal (Pt, Rh, and Pd) were studied. For O_2 and H_2 oxyreductions, the limiting amount of the removable oxygen in ceria was also measured as a function of temperature by temperature-programmed reduction (TPR). After the reduction by H_2 at 500°C, the amount of the restorable oxygen (restored at 0 and 500°C) in some CeO_2/Al_2O_3 samples were measured as a function of CeO_2-loading by selective oxygen chemisorption.

EXPERIMENTAL

Catalyst Preparation

CeO_2(1) was purchased from Alfa Chemical Company with a nominal purity of 99.9%. It was calcined at 800°C for 18 h. CeO_2(2) was prepared by decomposing $(NH_4)_2\ Ce(NO_3)_6 \cdot 6H_2O$ and calcining the resultant oxide at 800°C for 3 h. The surface areas of CeO_2(1) and CeO_2(2) as determined by Kr adsorption were 1.0 and 9.9 m^2/g, respectively. Alumina suspensions (Alon-30D from Cabot Corp. and Alumina-C powder from Kaiser) were dried at 250°C, calcined at 600°C, sieved, and the portion between 35 and 100 mesh was used as support for the catalyst. The BET areas were 80 and 150 m^2/g for Alon-30D and Kaiser Alumina-C, respectively.

The CeO_2/Al_2O_3 catalysts were prepared by wetting the Al_2O_3 with a sufficient amount of $Ce(NO_3)_3$ aqueous solution of desired concentration. The wet Al_2O_3 was dried and decomposed slowly under a heat lamp followed by calcination at 500 to 800°C for 16 h. Its composition was determined by both the amount and concentration of the solution used, and by the weight gain after calcination.

The samples containing precious metals (Pt, Pd, or Rh) were prepared by a conventional impregnation method. The supports were CeO_2, Al_2O_3, and CeO_2/Al_2O_3 of various compositions. An amount of the precious metal salt solution required to completely wet the support was used. The samples were dried slowly under a lamp and heated stepwise at increasing temperatures for 4 h or more at 600, 700, 800, and 900°C. Portions were taken after each step and used for the oxygen storage and oxidation activity tests. The concentration of precious metal (PM) in the final catalysts was calculated from the amount and the concentration of the PM salt solution used. The source materials were $PdCl_2$, H_2PtCl_6, and $Rh(NO_3)_3$.

Measures of Oxygen Storage Capacity

We have examined the incorporation (or removal) of oxygen from samples of unsupported ceria, ceria supported on γ-Al_2O_3, and of such supported samples containing the precious metals. As could be expected, the extent of the oxyreduction process and its rate are dependent on the state of the dispersion of the ceria and on the presence and dispersion of precious metal components and also on the temperature and partial pressure of the gaseous agents. This work examines this dependence using several experimental approaches.

We are interested in establishing the widest "limiting" amount of the transferable oxygen attained by prolonged reduction at temperatures attainable in the automotive exhaust, say up to 900°C. This was measured by temperature-programmed reduction (TPR). We will designate this amount, which is the largest from among the various quantities in our work, as TPR-O_2 and present in units of micromoles O_2/micromoles CeO_2 in the sample. We will employ the same units, for the sake of easy comparison, for all the other measurements of oxygen transfer as well.

The second measurement is that of oxygen chemisorption on prereduced samples. Clearly, this measurement provides us with a yardstick of those sites available on the surface of our catalyst samples. These sites will be the most easily accessible during the rapid oscillation in the exhaust composition of the engine exhaust. Since chemisorption is an activated process, we have carried out the measurements both at 0 and 500°C. The

second measurement is more representative of the pool of available *surface* sites for oxygen transfer available during actual operation of the catalysts, since the temperature of 500°C is quite representative (even somewhat of the higher end) of the operation range in actual use. The chemisorbed amount provides a "limit" which may be approached to a lesser or greater extent during actual cycling, while the previous total amount of transferable oxygen measured by TPR is not accessible, most of it being in the bulk. The differences between the oxygen transferable in TPR experiments and in chemisorption will be expected to widen with the increase in ceria-loading.

The third measure was the amount of oxygen transferred in a pulsed regime simulating the oscillations which the exhaust gas may undergo. Two measures were used here: one was the total amount of CO oxidized in a series of CO pulses following an oxygen pulse until no more CO oxidation was observed, and the other was the amount of CO oxidized in only one CO pulse following an oxygen pulse. The former will be designated "Oxygen Storage Capacity, Complete" or OSCC. The latter, which should be closest to what can be expected to be utilized in actual operation, will be designated "Oxygen Storage Capacity" or OSC. The detailed measurement procedure will be given below in the "Pulse Injection" part.

Chemisorption Measurements

Oxygen uptake was measured at 0 and 500°C in a conventional constant-volume adsorption apparatus equipped with a Texas Instrument Model 145 precision gauge linked to a fused-quartz Bourdon spiral. Before the measurements, each sample was prereduced by flowing H_2 at 500°C for 2 h. The hydrogen was purified by passage over an Engelhard DEOXO Pd catalyst and a 4-Å molecular sieve at 78°K. Research grade oxygen was used without further purification.

Temperature-Programmed Reduction (TPR)

The apparatus and procedure used for the TPR study have been described in full before (*14*). In these measurements, a H_2(15%)–Ar(85%) gas mixture was used as a reducing gas and the temperature rise of the catalyst was controlled at a constant rate of 10°C/min.

Pulse Injection

The catalyst sample was placed in a Pyrex or quartz U-tube reactor which was kept at a desired temperature with a tube furnace. The carrier gas, He, was passed continuously through the sample at a rate controlled by a Matheson Model 8240 Flow Controller. O_2–He and CO–He mixtures in the concentration range of 1–2% were supplied from Matheson Gas Products Company. They were injected into the carrier gas stream through a pair of Carle valves each connected to a gas-sampling loop of calibrated volume. The valves were arranged in series so that only one loop could be opened to the sample at a time. The individual injections were separated by helium purges of 20–30 s duration. Therefore, the total time elapsed for a complete oxyreduction cycle is 40–60 s although the actual contact time of the pulse was ~1 s. The valve switches were operated manually so that the sequence and timing could be changed at will. The conditions of the experiments were such that the volume of the pulse of 1% O_2 in He or 1% CO in He was very much larger than the catalyst volume. For example, the pulse volume for the He + 1% O_2 used for many of the runs was 2.55 cm^3 and for He + 1% CO twice this. The catalyst volume was ~.04 cm^3. During a pulse experiment, He is passed over the catalyst at 200 cm^3/min.

The composition of the inlet and outlet gas streams was monitored with a CEC 21 Mass Spectrometer operated in the continuous flow mode. The area under the mass

peak, was measured with a simple condenser integrator. The difference in the mass peak area of the inlet and exiting gas of each injected pulse is the measure of O_2 or CO uptake or of CO_2 produced. At equilibrium, the value of O_2 uptake is deemed to be the oxygen storage capacity of the catalyst under the particular set of reaction conditions used.

As a standard procedure, the catalyst was heated in He flow at 500°C or above for at least 30 min, then it was completely oxidized by O_2 by injecting pulses of He containing 1% O_2 successively until a 100% breakthrough was attained. It was then cooled to the reaction temperature and alternating injections were made of pulses of He with 1% CO followed by pulses of He with 1% O_2 until there was established an apparent equilibrium breakthrough for both gases. At least five measurements of the CO and O_2 uptake and the CO_2 produced were determined for each sample. The reproducibility was of the order of 0.01 μmol. The amount of O_2 uptake in each pulse injection was designated OSC, as noted above.

At the end of each run, the sample was treated with a series of successive injections of He with 1% CO until a constant breakthrough ≥95–98% was reached. The sample was then returned to the O_2-saturated state with a series of successive injections of He containing 1% O_2. The total oxygen uptake for the series is the measure of the cumulative oxygen storage capacity (OSCC).

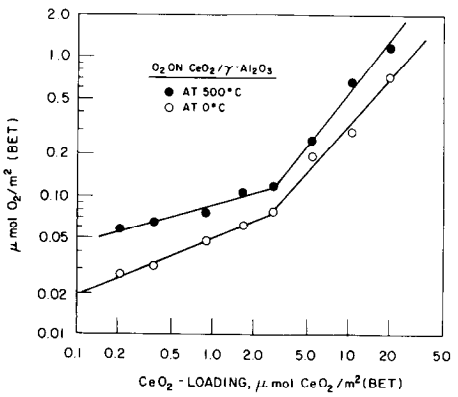

FIG. 1. Irreversible oxygen uptake as a function of CeO_2 loading. ●, at 500°C; ○, at 0°C. All samples are precalcined at 500°C for 16 h followed by reduction in H_2 at 500°C for 2 h.

TABLE 1

Irreversible Oxygen Chemisorption and Oxygen Removal (TPR–OX) on Samples of CeO_2/Al_2O_3

CeO_2 concentration		O_2 chemisorption (μmol O_2/μmol CeO_2)		TPR–OX (μmol O_2/μmol CeO_2)
% CeO_2	μmol CeO_2/m^2 (BET)	0°C	500°C	
.48	.21	.13	.27	.27
.83	.37	.09	.18	.25
2.04	.90	.05	.09	.24
3.72	1.65	.04	.06	.24
6.14	2.72	.03	.05	.23
11.69	5.35	.04	.05	.21
21.63	10.65	.03	.06	.22
35.38	20.03	.04	.06	.20

RESULTS

1. Chemisorption Measurements

Total and reversible adsorption isotherms of oxygen (up to 100 Torr pressure), at 0 and 500°C on eight CeO_2/γ-Al_2O_3 samples of various CeO_2 concentration were measured, each following the reduction by flowing hydrogen at 500°C for 2 h. The reversible adsorption was measured following the total adsorption after the same sample was degassed at the same temperature for 1/2 h. The difference between the total and reversible adsorption was the irreversible part which was used for the comparison of (i) the amount of O_2 uptake in Fig. 1 and (ii) the stoichiometric ratio, O_2/CeO_2, in Table 1.

Each of the logarithmic plots of O_2 uptake as a function of CeO_2-loading, (Fig. 1) consists two linear sections which intersect at about 2.5 μmol CeO_2/m^2(BET). We attribute this phenomenon to the presence of two phases of CeO_2 on γ-Al_2O_3 (*14–16*). At low CeO_2 concentrations (≤2.5 μmol CeO_2/m^2[BET]), all CeO_2 is present in the dispersed phase and oxygen uptake increases moderately with CeO_2-loading. The dis-

persed phase reaches saturation at about 2.5 μmol/m^2 (BET) beyond which the excess CeO_2 aggregates to form small particles and oxygen uptake rises faster with CeO_2 loading.

The oxygen chemisorption is given in Table 1 and, as expected, the results indicate that the uptake of O_2 per unit weight of ceria decreases with loading because of the decreased ceria dispersion. It becomes virtually constant at a loading of a few percents CeO_2, actually even before the saturation concentration of the dispersed phase is attained. In a separate series of supported ceria, in the 9–27 wt% CeO_2 range, samples which were calcined at 800°C for 16 h, the particle size of ceria was measured by X-ray diffraction and found to be virtually constant at the range 55 to 67 Å. The ratio of exposed CeO_2 to those in the bulk for this range is ~0.45. We see that only a small fraction of the surface ceria is accessible to oxygen at 0°C and a larger fraction at 500°C. This indicates that the oxygen adsorption on ceria is strongly activated as was already obvious from Fig. 1.

2. *Temperature-Programmed Reduction*

The hydrogen uptake as a function of temperature by unsupported ceria is shown on Fig. 2. The results for three different samples of which one was subjected to further reoxidation are shown on the figure. Only two peaks are noted in all traces, a large one at ~750°C and a smaller one at ~500°C. The area of the low-temperature peak with respect to that of the high-temperature peak is considerably lower for the low-surface area sample, trace A.

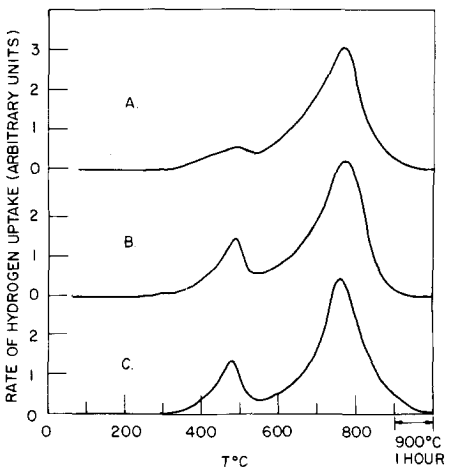

FIG. 2. Rate of H_2 uptake as a function of temperature in the TPR of CeO_2 samples. (A) CeO_2(1), BET area: ~1 m^2/g. (B) CeO_2(2), BET area: 10 m^2/g. (C) Same as in (B), reoxidized at 200°C after the previous reduction.

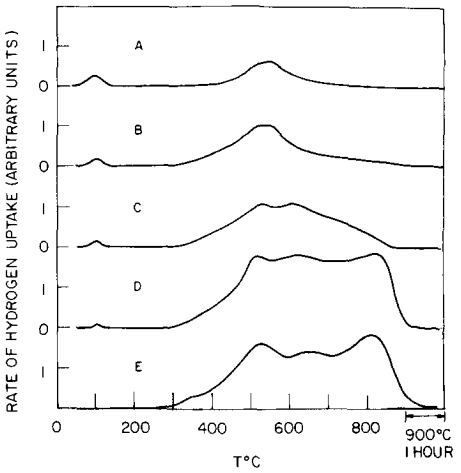

FIG. 3. Rate of H_2 uptake as a function of temperature in the TPR of CeO_2/Al_2O_3 samples. (A) 0.83% CeO_2/Al_2O_3; (B) 2.04% CeO_2/Al_2O_3; (C) 6.14% CeO_2/Al_2O_3; (D) 11.7% CeO_2/Al_2O_3; (E) 21.6% CeO_2/Al_2O_3.

Figure 3 shows the TPR traces of the supported ceria samples in ascending order of CeO_2 loading. The following features are observed: The low-loading samples show the low-temperature peak seen in Fig. 2 although shifted upscale to ~550°C. A more complex structure is seen in the higher loading samples, one can discern three peaks of oxygen uptake, although considerable overlap between them is noted and the resolution is not at all sharp. In addition, there is a small peak in the low temperature range (~100°C) which diminishes with CeO_2 loading. The total amount of oxygen removed in the course of the TPR is of the range of 0.20–0.27 μmol O_2/μmol of CeO_2. These data are incorporated into Table 1 as the last column.

The oxygen removed in the TPR corre-

sponds roughly to one-electron transfer per CeO_2. This indicates that during the TPR the whole amount of ceria in the supported samples undergoes the oxyreduction $Ce^{4+} \leftrightarrows Ce^{3+}$. The same is true of the unsupported ceria samples, both of the high-, and low-surface area variety.

The effect of the noble metals on the TPR of ceria is shown in traces A and B of Fig. 4. Comparing these spectra with those of Fig. 2, we note that the presence of noble metals does not affect the high-temperature reduction peak but lowers and splits the low-temperature (at 450°C) reduction peak. Below 500°C we see both in the presence of Rh or Pt a multiplicity of peaks (*5*) instead of the single peak in the case of the unsupported ceria (Fig. 2). In trace C of Fig. 4, the effect of Pt on TPR of the Al_2O_3-supported CeO_2 is similar. While the presence of Pt lowers and splits the low-temperature peak, it does not affect the middle- and the high-temperature peaks at 650 and 870°C, respectively.

Figure 5 shows TPR traces of a high-loading CeO_2/γ-Al_2O_3 sample (19.7% wt CeO_2) after reoxidation treatment at different temperatures of samples completely reduced at 900°C. The room temperature pre-

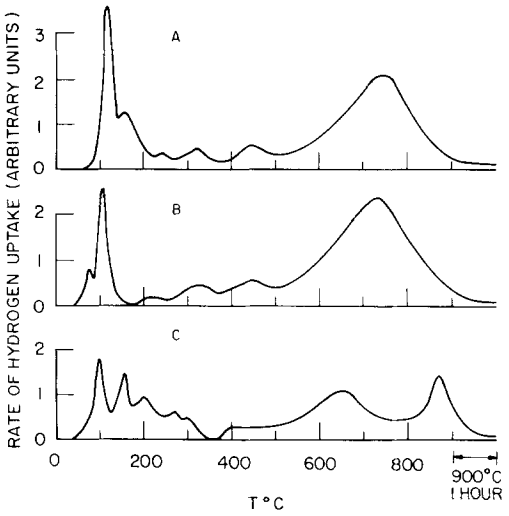

FIG. 4. Rate of H_2 uptake as a function of temperature in the TPR of (A) 3% Rh/CeO_2; (B) 3% Pt/CeO_2; (C) 2.4% $Pt/22.8\%$ CeO_2/Al_2O_3.

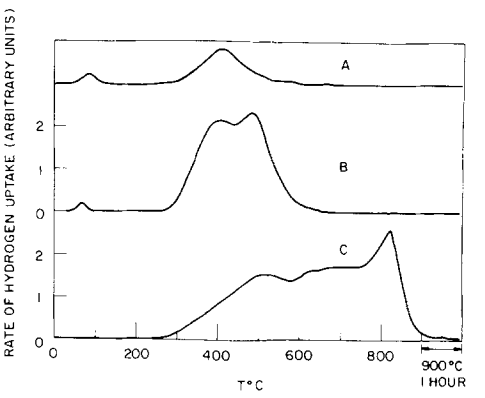

FIG. 5. Rate of H_2 uptake as a function of temperature in the TPR of the 21.6% CeO_2/Al_2O_3 which was reduced at 900°C and then reoxidized at (A) 25°C, 10 min; (B) 500°C, 16 h; (C) 850°C, 2 hr.

oxidation restores the low-temperature peak (100°C) and the peak at 400°C. The reoxidation at 500°C increases this peak also showing its splitting. Finally, the reoxidation at 850°C, restores, in broad resemblance, the behavior noted in Fig. 3, trace E. The TPR spectra in the figure show that the ease of removal of oxygen from the bulk of the supported ceria is dependent on the conditions, in particular the temperature, of the preceding reoxidation itself. This dependence on the temperature for reoxidation is in good agreement with the chemisorption data (Fig. 1 and Table 1) which indicates that the reoxidation of reduced ceria is a highly activated process. In essence we are dealing with a metastable defect and nonstoichiometric (Ce^{3+}–Ce^{4+}) material. As the oxidation proceeds to completion, the structure becomes more ordered and more difficult to reduce.

Pulse Injection Measurements

These measurements, as indicated before, are more closely related to the actual enhancement of the "oxygen storage" capacity by the incorporation of ceria than the work discussed before. This capacity is influenced by several operating parameters: two temperatures, that of the pretreatment and that of actual pulsing experiment; the

concentration of the gaseous reactant and finally the presence of precious metals.

Hydrogen is known to be a more effective reducing agent than CO particularly in the presence of PM. The actual exhaust gas contains hydrogen in proportion of between 1/4 and 1/3 that of CO. The implication of this is that if in actual exhaust the pulses are of the same frequency (~1 Hz) the extent of storage capacity will not be less than observed in these experiments.

The data on the pulsing results are given in the following four tables. Note that the oxygen storage capacities related to ceria content are by ~2 orders of magnitude lower than total removable oxygen as measured by TPR.

(*1*) *Effect of pretreatment temperature.* The effect of pretreatment temperature was measured only for the samples of unsupported CeO_2 and noble metals on CeO_2. The data are presented in Table 2, from which one can notice a general decrease in the storage capacity when going from 600 to 800°C in the pretreatment temperature. This behavior is observed for all the samples in Table 2. Since, one can expect that in the actual catalyst usage during normal operation the catalyst will be periodically exposed to temperatures ~800°C, this treatment temperature was used for the calcination of most of the supported catalysts used in the pulse-injection experiments.

(*2*) *Effect of pulsing temperature.* It was observed during the chemisorption experiments (Fig. 1 and Table 1) that the adsorption of oxygen is an activated process. Similarly in the data of Table 2 it is already apparent that with the increase of pulsing temperature more oxygen can be stored during a given single pulse and also in the cumulative storage experiment. Although the data in Table 2 indicates that at the upper temperature of 500°C the limit has not yet been reached it is this temperature range which is of most interest. Table 3 gives the results of pulsing experiments as a function of temperature on catalysts supported on alumina with the storage capacity referred again to the ceria content. The precious metal components of the catalyst are by themselves, at the surface, capable of undergoing oxyreduction and we will subsequently try to distinguish between these contributions. The data in Table 3 are for the system as a whole. The following observations can be deduced from the data in Table 3. First, with increasing temperature of pulsing a larger proportion of the available storage is being utilized. Further, the difference between the limiting (cumulative) storage capacity and that achievable in

TABLE 2

Effect of Pretreatment and Pulsing Temperatures on Oxygen Storage Capacity (μmol O_2/μmol CeO_2) × 10^2

Sample	Pretreatment temperature (°C)	Pulsing temperature (°C)					
		300		400		500	
		OSCC	OSC	OSCC	OSC	OSCC	OSC
CeO_2	600	—	—	0.18	0.06	0.44	0.19
	800	—	—	—	—	0.33	0.14
0.058% Pd/CeO_2	600	0.14	0.08	0.31	0.20	0.41	0.31
	800	0.15	0.07	0.32	0.18	0.38	0.25
0.094% Pt/CeO_2	600	0.16	0.06	0.36	0.20	0.45	0.26
	800	—	—	0.31	0.18	0.36	0.21
0.04% Rh/CeO_2	600	0.29	0.18	0.41	0.33	0.49	0.32
	800	—	—	0.35	0.10	0.29	0.19

TABLE 3

Effect of Pulsing Temperature on Oxygen Storage Capacity in Alumina-Supported Catalysts (μmol O_2/μmol CeO_2) × 10^2

Sample	Pulsing temperature (°C)					
	300		400		500	
	OSCC	OSC	OSCC	OSC	OSCC	OSC
20% CeO_2/Al_2O_3	—	—	—	0.03	0.87	0.17
0.153% Pd/20% CeO_2/Al_2O_3	0.53	0.22	1.56	0.87	2.57	1.77
0.300% Pt/23% CeO_2/Al_2O_3	1.11	0.57	1.66	1.44	2.09	1.49
0.155% Rh/20% CeO_2/Al_2O_3	0.62	0.19	1.23	0.78	1.83	1.11

Note. All catalysts calcined at 800°C.

a single pulse is narrowed, especially for the catalysts containing noble metals, 60–70% of the oxygen storage is utilized in a single pulse. Because the atomic concentration of three noble metals is roughly the same, there is only a slight difference (if any) in the individual effect of the noble metals.

(*3*) *Effect of partial pressures of oxygen and carbon monoxide.* By varying the partial pressure of O_2 and CO in the pulse injection system, their effects on OSC and OSCC were examined. The results in Table 4 show that for the reactions over CeO_2(2) and 20% CeO_2/Al_2O_3 samples at 500°C, the change of partial pressure of oxygen from 1 to 2% does not change significantly the OSC and OSCC values while the increase in partial pressure of CO from 1 to 2% leads to a large increase of both OSC and OSCC. This is because both OSC and OSCC are measured by CO oxidation which is a slower step and is a temperature- and CO pressure-dependent process. OSCC values are the total amount of the available oxygen under that condition and, therefore, are affected by the CO pressure.

(*4*) *The effect of precious metal and CeO_2 concentration.* The presence of Pt, Pd, and Rh generally increases the OSC and OSCC values of CeO_2. The corrected OSC and OSCC values in Table 5 are those after the subtraction of the OSC due to the precious metal itself. Compared with the unsupported CeO_2(2) sample (of which the OSCC and OSC values at 500°C are 0.33 and 0.14, respectively) the increase is small for the unsupported but large for the Al_2O_3-supported sample. This indicates that the effect of precious metal is only on the surface CeO_2 or on the dispersed phase of CeO_2 on Al_2O_3. With the concentration range of 0.03 to 0.3% PM and 8.9 to 23% CeO_2, the dependence of the corrected OSCC and OSC values on concentrations of both components is small.

TABLE 4

Effect of O_2 and CO Partial Pressures on OSCC and OSC (μmol O_2/μmol CeO_2) × 10^2, at 500°C

Sample	P_{O_2} (%)	P_{CO} (%)	OSCC	OSC
CeO_2(2)	1	1	.44	.21
	2	1	.40	.19
	2	2	.47	.32
20% CeO_2/Al_2O_3	1	1	1.1	0.30
	2	1	0.9	0.28
	2	2	1.5	0.43
0.094% Pt/CeO_2	1	1	0.43	0.25
	1	2	0.47	0.30
0.042% Pd/CeO_2	1	1	0.35	0.21
	1	2	0.44	0.29
0.04% Rh/CeO_2	1	1	0.30	0.24
	1	2	0.31	0.31
0.05% Pt/23% CeO_2/Al_2O_3	1	1	1.79	1.47
	2	2	2.43	1.86
0.021% Pd/12% CeO_2/Al_2O_3	1	1	1.70	1.22
	2	2	2.53	1.75
0.03 Rh/20% CeO_2/Al_2O_3	1	1	1.59	0.67
	2	2	1.51	0.67

TABLE 5

Effect of Precious Metal Concentration on Oxygen Storage Capacity in Pt-, Pd-, and Rh-Containing Catalysts at 500°C

Sample	OSCC $\left(\frac{\mu\text{mol } O_2}{\mu\text{mol } CeO_2} \times 10^2\right)$	OSC	Corrected OSCC $\left(\frac{\mu\text{mol } O_2 - 0.5 \times \mu\text{mol PM}}{\mu\text{mol } CeO_2} \times 10^2\right)^a$	Corrected OSC
0.094% Pt/CeO_2	0.36	0.21	0.32	0.17
0.23% Pt/CeO_2	0.48	0.26	0.38	0.16
0.05% $Pt/23\%$ CeO_2/Al_2O_3	2.02	1.48	1.92	1.38
0.3% $Pd/23\%$ CeO_2/Al_2O_3	2.09	1.49	1.51	0.94
0.058% Pd/CeO_2	0.38	0.25	0.34	0.21
0.14% Pd/CeO_2	0.44	0.25	0.33	0.14
0.05% $Pd/8.9\%$ CeO_2/Al_2O_3	2.55	2.0	2.1	1.6
0.2% $Pd/8.9\%$ CeO_2/Al_2O_3	4.0	3.4	2.3	1.7
0.04% Rh/CeO_2	0.29	0.19	0.26	0.16
0.03% $Rh/23\%$ CeO_2/Al_2O_3	2.02	1.48	1.92	1.38
0.16% $Rh/20\%$ CeO_2/Al_2O_3	2.09	1.49	1.51	0.94

[a] The correction equation assumes that each micromole of PM has 0.5 μmol O_2 in OSCC and OSC.

DISCUSSION

Below 1000°C, ceria can be reduced by H_2 only to Ce_2O_3 (*18–20*). The total oxygen storage of the catalyst depends on ceria-loading. For the practical use in the automotive exhaust treatment system, the ceria-loading is about 20% with respect to alumina which, in monolith catalysts, is equivalent to 2% by weight of the catalyst.

The pulse injection data (Tables 2–5) show the dependence of OSC on pretreatment temperature, pulsing temperature, partial pressure of reactants, and on the presence of precious metals. An increase of precalcination temperature from 600 to 800°C (Table 2) lowered the OSC for CeO_2 by ~25%, for both Pd/CeO_2 and Pt/CeO_2 by ~20%, and for Rh/CeO_2 by ~40%.

The dependence of OSC on pulsing temperature is shown in both Tables 2 and 3. In CeO_2 (Table 2), no OSCC or OSC is found at a pulsing temperature of 300°C, negligible amount at 400°C, and a considerable amount at 500°C. For Pt/CeO_2, Pd/CeO_2, and Rh/CeO_2 samples, both OSCC and OSC values are much higher when compared with CeO_2 at 300 and 400°C. This indicates that the presence of a precious metal facilitates both the restoration of the surface oxygen anions and their removal by CO at lower temperatures. Note that in $PM/CeO_2/Al_2O_3$ (Tables 3 and 5), the OSCC and OSC values are much higher than in CeO_2/Al_2O_3 and PM/CeO_2 even at 500°C. We attribute this increase to the $PM–CeO_2$ interaction which not only lowers the reduction temperature for CeO_2 but also increases the dispersion of CeO_2 on alumina.

The TPR traces for the reduction of CeO_2 and CeO_2/Al_2O_3 (Figs. 2 and 3) are very similar to the TPR traces for the reduction of MoO_3 and MoO_3/Al_2O_3 (*16*), save for the fact that up to 900°C while MoO_3 can be reduced to metallic Mo, CeO_2 can be reduced only to Ce_2O_3. Similar to the interpretation for the MoO_3 reduction (*16*), the presence of two peaks in TPR traces of Fig. 2 is attributed to the existence of two types of oxygen anions in CeO_2. A surface capping oxygen anion which attaches to a surface Ce^{4+} ion in an octahedral coordination is reducible at about 500°C. A bulk oxygen anion which is bonded to two Ce^{4+} ions in the bulk ceria is reducible at 750°C. The relative intensity of these two peaks is af-

fected by the surface area of ceria (Fig. 2). The TPR traces for the alumina-supported ceria are more complicated (Fig. 3). A small peak at 100°C in traces A, B, C, D of Fig. 3 which diminishes when CeO_2 concentration increases can be attributed to the small amount of removable oxygen anions on the bare amorphous Al_2O_3 sites. Such removable oxygen anions on amorphous alumina were noticed during degassing at ~500°C (*21, 22*). We observe such anions only on the CeO_2/Al_2O_3 samples of low CeO_2-loading. They vanish with CeO_2-loading. A larger peak at 530°C in traces A, B, C, D, E of Fig. 3 is attributed to the reduction of surface capping oxygen anions on the supported ceria. The bulk oxygen anions which are absent in the supported ceria of low concentration (traces A and B of Fig. 3) begin to appear in samples of higher ceria concentration (trace C). The 600°C peak in trace C of Fig. 3 is associated with the reduction of bulk oxygen anion. As ceria concentration increases from 6.14 to 21.6 wt%, this peak shifts upscale from 600 to 650°C (trace E), which is lower than the 750°C peak for bulk oxygen anions in the unsupported ceria (Fig. 2). This upscale temperature shift from 600 to 750°C indicates probably the particle size dependency in the reduction of bulk oxygen anions in both the supported and unsupported ceria. Another peak at 850°C which appears together with the 650°C peak in the samples of high ceria concentration (Fig. 3) is attributed to the reduction of the shared oxygen anions (shared between Ce^{4+} and Al^{3+} ions) in the interface between the bulk ceria and alumina. While the capping oxygen anions are present in all CeO_2 and CeO_2/Al_2O_3 samples, bulk and shared oxygen anions are found only in CeO_2 and in CeO_2/Al_2O_3 of high CeO_2-loading. The absence of bulk oxygen anions in traces A and B of Fig. 3 indicates that all CeO_2 in these samples are present in the dispersed phase. These results are in good agreement with the chemisorption data (Fig. 1) which shows the appearance of CeO_2 bulk at CeO_2-loading of greater than 2.5 μmol CeO_2/m^2 (BET) or ~6% CeO_2/Al_2O_3. The lack of a 850°C peak in traces A and B of Fig. 3 does not mean the absence of shared oxygen anions in these samples. It indicates that such shared oxygen anions in the dispersed phase cannot be further removed even at high temperatures since the removal of capping oxygen has already reduced the Ce^{4+} ion in the dispersed phase to the limit oxidation state of Ce^{3+}. Thus, for samples of low-CeO_2 loading, complete reduction by H_2 is attainable at 500°C and no further reduction is possible even at higher temperatures.

The TPR data for the removal of oxygen anions from PM/CeO_2 and $PM/CeO_2/Al_2O_3$ samples are shown in Fig. 4. In traces A and B of Fig. 4, the peaks which appear at <150°C are associated with the reduction of the supported Rh and Pt oxides (*15, 17*). In the temperature region between 150 and 500°C, one notes a multiplicity of peaks associated with the presence of precious metal on CeO_2 or CeO_2/Al_2O_3. At present, we do not have a proven assignment for the oxygen species associated with each one of these peaks. We presume that the bonding of the capping oxygen anions of ceria (the peaks at 500°C in Figs. 2 and 3) has now been differentiated in several ways by interaction with PM of various possible states of aggregation during the reduction. Beyond this assumption no further speculation can add to our understanding. In the higher temperature region above 500°C (Fig. 4) the TPR traces are unaffected by the presence of precious metal, indicating the absence of interaction from both the bulk oxygen anions and the shared oxygen anions of ceria with the precious metal.

The restoration of oxygen on CeO_2/Al_2O_3 samples after a reduction by H_2 at 500°C was measured by chemisorption at 0 and 500°C (Table 1). It indicates that the oxygen resotration is faster than reduction by H_2 and is dependent on temperature and concentration of CeO_2 on Al_2O_3. At 500°C, the amount of oxygen restored is twice the amount of oxygen at 0°C. The amount of

oxygen restored in units of micromoles O_2/micromoles CeO_2 is highest at the lowest concentration of CeO_2. It decreases as the CeO_2 concentration increases and levels off after the concentration reaches the saturation of dispersion at about 2.5 μmol CeO_2/m^2 (BET) (Fig. 1).

The restoration of oxygen on a 21.6% CeO_2/Al_2O_3 sample at temperature of 25 to 950°C after a prereduction by H_2 at 900°C was measured by TPR (Fig. 5). After the first reduction at 900°C, the oxygen was restored at 25°C and trace A shows the presence of some new oxygen species at 400°C but no capping oxygen anion. After a second reduction at 900°C, oxygen was restored at 500°C and trace B shows again the new oxygen species at 400°C and some capping oxygen anions at 500°C. Only after the third reduction at 900°C and followed by restoration at 850°C, the new oxygen species does not appear again and all other three types of oxygen anions reappear. Apparently, complete reoxidation of Ce_2O_3 to CeO_2 on Al_2O_3 requires a temperature of about 850°C.

During the repeated reduction at 900°C (Fig. 5), some surface structure changes of CeO_2 on Al_2O_3 are observed. Note that after the reduction at 900°C and reoxidation at 25°C for the 21.6% CeO_2/Al_2O_3 sample, the low-temperature peak at ~100°C reappears (compare trace A of Fig. 5 with trace E of Fig. 3). The reduction at 900°C may cause the sintering or aggregation of the dispersed CeO_2 during reduction of CeO_2 to Ce_2O_3 and consequently restores some bare amorphous Al_2O_3 sites for oxygen adsorption. Reoxidation at 500 and 850°C can rearrange surface oxygen anions and the low-temperature peak (~100°C) disappears. After the reduction and reoxidation at 850°C, the high-temperature (850°C) peak increases at the expense of the 450°C peak, indicating some conversion of capping oxygen anions to the shared oxygen anions (trace C, Fig. 5) during the repeated reduction and oxidation processes.

Although there are several possible structures for the new surface oxygen species mentioned above, such as

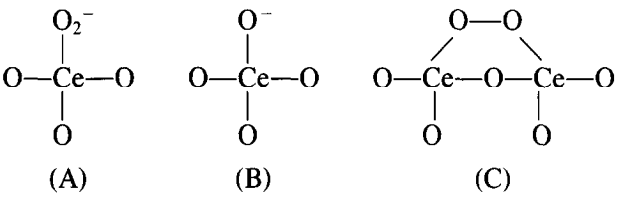

(A) (B) (C)

only species (A) was formed and identified on a supported and reduced CeO_2 sample (*23*). Species (A) is tentatively assigned to be the new surface oxygen species which is metastable, can be converted to the capping, bulk, and shared oxygen anions at about 850°C, and is readily available for the redoxy reaction at <500°C.

ACKNOWLEDGMENTS

The authors are indebted to Dr. J. T. Kummer and Dr. E. C. Su for many helpful discussions and to Dr. M. Shelef and Dr. H. S. Gandhi for a critical review of the manuscript and helpful suggestions. Mr. C. R. Peters supplied the XRD results and Mr. W. L. H. Watkins helped in the TPR experiments.

REFERENCES

1. Kummer, J. T., "Proceedings of Energy Combustion Science," Vol. 6, p. 177. Pergamon, Ltd, Great Britain, 1980.
2. Gandhi, H. S., Piken, A. G., Stepien, H. K., Shelef, M., Delosh, R. G., and Heyde, M. E., SAE Preprint 770196, Detroit, Mich., 1977.
3. Hegedus, L. L., Summers, J. C., Schlatter, J. C., and Baron, K., General Motors Research Publication GMR-2730, June 1978.
4. Su, E. C., and Montreuil, C., Ford Technical Report, SR-78-64, July 1978.

5. Su, E. C., and Rothschild, W. G., Ford Technical Report, SR-79-105, Sept. 1979.
6. Peters, M. S., and Wu, J. L., *Atmos. Environ.* **11,** 459 (1977).
7. Summers, J. C., and Ausen, S. A., *J. Catal.* **58,** 131 (1979).
8. Kummer, J. T., Yao, Y. F. Yu, and McKee, V., SAE Paper 760143, Detroit, Mich., 1976.
9. Kozlov, N. S., Senkov, G. M., Zaretskiti, M. V., Davidovskaya, A. M., and Palei, N. V., *Dokl. Akad. Nauk BUSSR* **18,** 621 (1974); *Chem. Abstr.* **81,** 127140 Y.
10. Sergey, F. J., Masellei, J. M., and Ernest, M. V., W. R. Grace Co. U.S. Patent 3,903,020 (1974).
11. Hindin, S. G., Engelhard Mineral and Chemical Co., U.S. Patent 3,870,455 (1973).
12. Masakazu, O., and Yoshizo, K., Hitachi Maxwell Ltd., Japanese Patent 76–17, 195 (1976).
13. Kim, G., *Ind. Eng. Chem. Prod. Res. Dev.* **21,** 267 (1982).
15. Yao, H. C., Japar, S., and Shelef, M., *J. Catal.* **44,** 392 (1976).
16. Yao, H. C., *J. Catal.* **70,** 440 (1981).
17. Yao, H. C., Sieg, M., and Plummer, H. K., Jr., *J. Catal.* **59,** 365 (1979).
18. Brauer, G., and Grandinger, H., *Z. Anorg. Allg. Chem.* **277,** 89 (1954).
19. Brauer, G., and Holtschmidt, *Z. Anorg. Allg. Chem.* **265,** 105 (1951).
20. Shedd, E. S., and Henrie, T. A., *in* "Rare Earth Research II" (K. S. Vorres, Ed.), p. 21–27. Science Publ., New York, 1964.
21. Hoang-Van, C., and Teichner, S. J., *J. Catal.* **16,** 69 (1970).
22. Hoang-Van, C., and Teichner, S. J., *J. Catal.* **16,** 75 (1970).
23. Che, M., Kibblewhite, J. F. J., Tench, A. J., Dufaux, M., and Naccache, C., *J. Chem. Soc. Faraday Trans.* **69,** 857 (1973).